Supporting Information for "Limitations in one-dimensional (an)elastic Earth models for explaining GPS-observed M_2 Ocean Tide Loading displacements in New Zealand"

B. Matviichuk[1], M. King[1],C. Watson[1], M. Bos[2]

[1]School of Geography, Planning, and Spatial Sciences, University of Tasmania, Hobart, 7001, Australia

[2]Instituto Dom Luiz (IDL), University of Beira Interior, Covilhã, Portugal

Contents of this file

1. Figures S1 to S10
2. Table S5
3. Table S6

Additional Supporting Information (Files uploaded separately)

1. Table S1. New Zealand GPS site name, network and coordinates (Table_S1.xlsx)
2. Table S2. New Zealand GPS-derived M_2 amplitudes and phases (Table_S2.xlsx)
3. Table S3. Australia GPS site name, network and coordinates (Table_S3.xlsx)
4. Table S4. Australia GPS-derived M_2 amplitudes and phases (Table_S4.xlsx)

0148-0227/21/$9.00

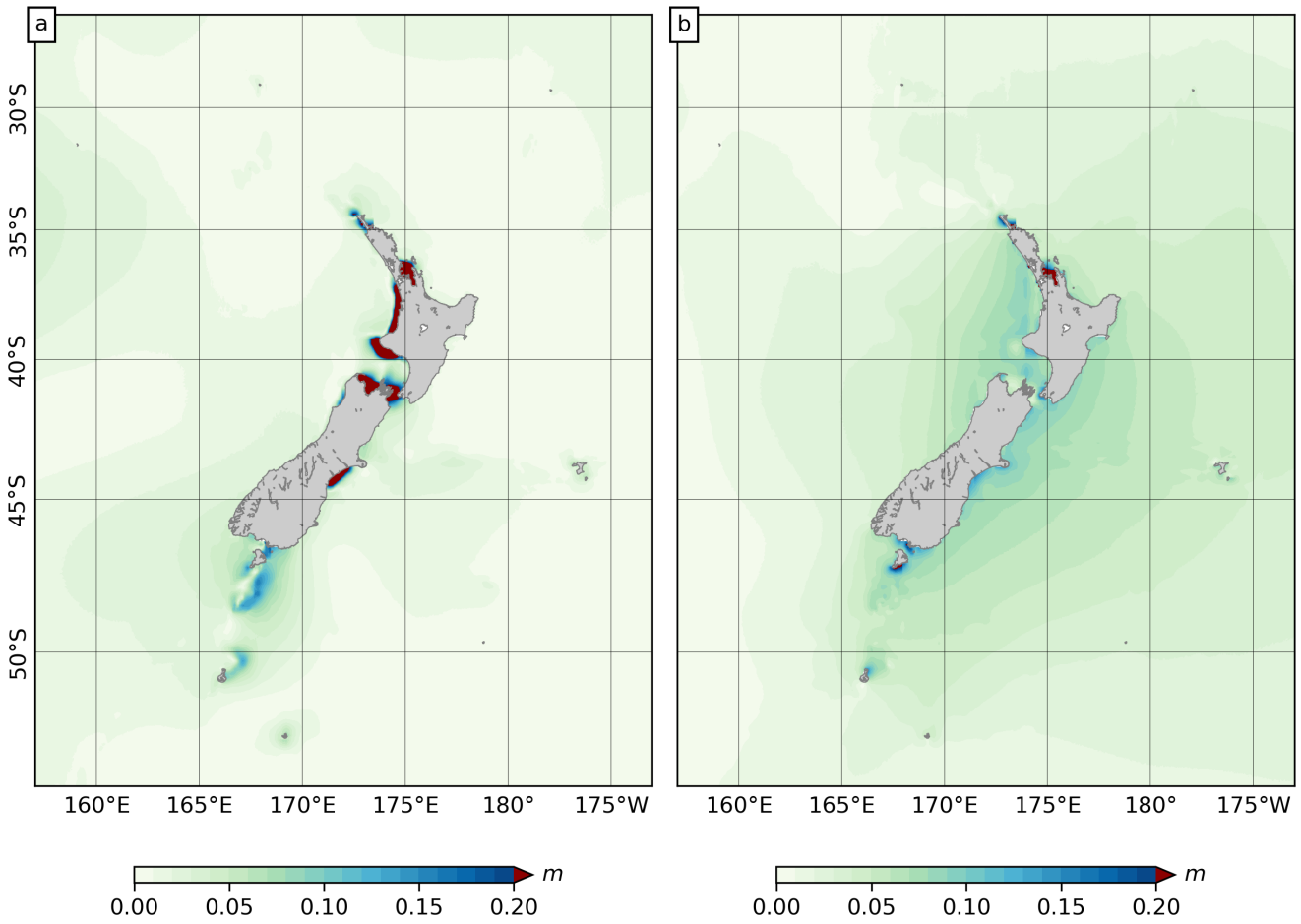

Figure S1. Vector differences between the mean model and FES2004 global tide model (a) and regional EEZ ocean tide model (b). Differences are concentrated in the shallow waters in the case of FES2004 while EEZ differences show the presence of uniform bias (∼0.1 m), which reduces away from the coast. Note the scale saturation above 0.2 m. The peak values are 1 m and 0.7 m for (a) and (b), located at the Hauraki Gulf in both cases.

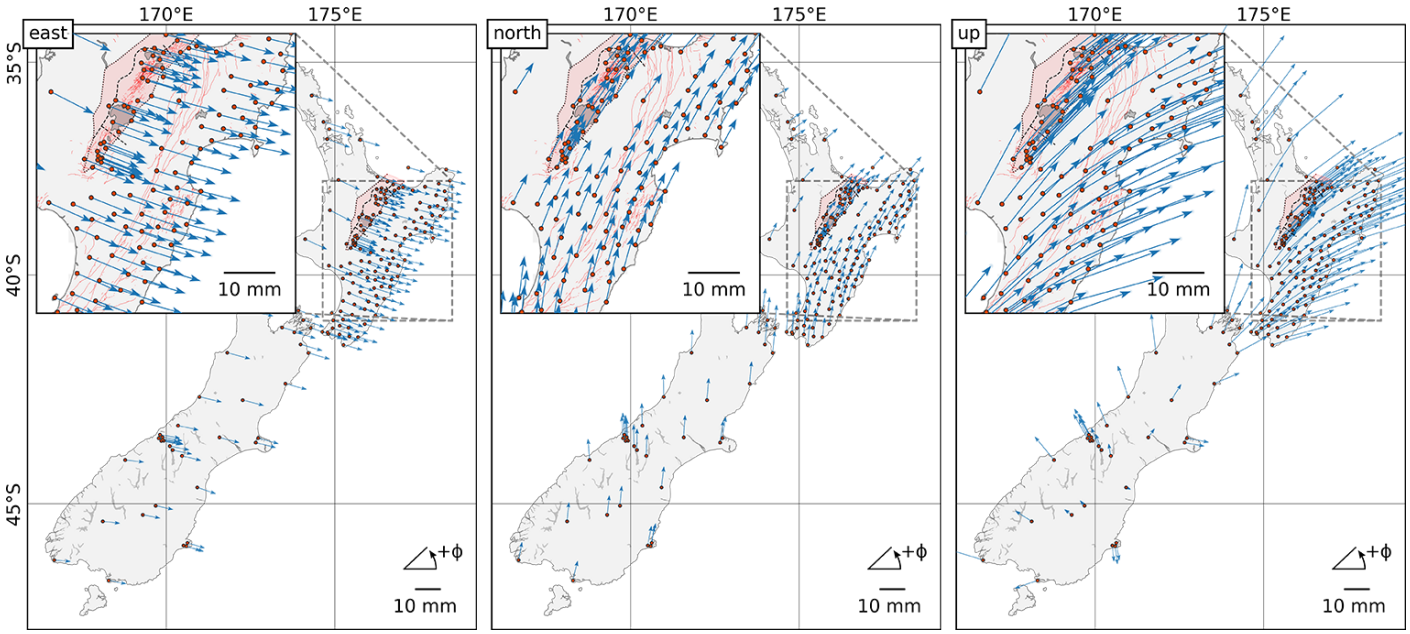

Figure S2. FES2004 restored GPS-derived ocean tide loading in the east, north and up components.

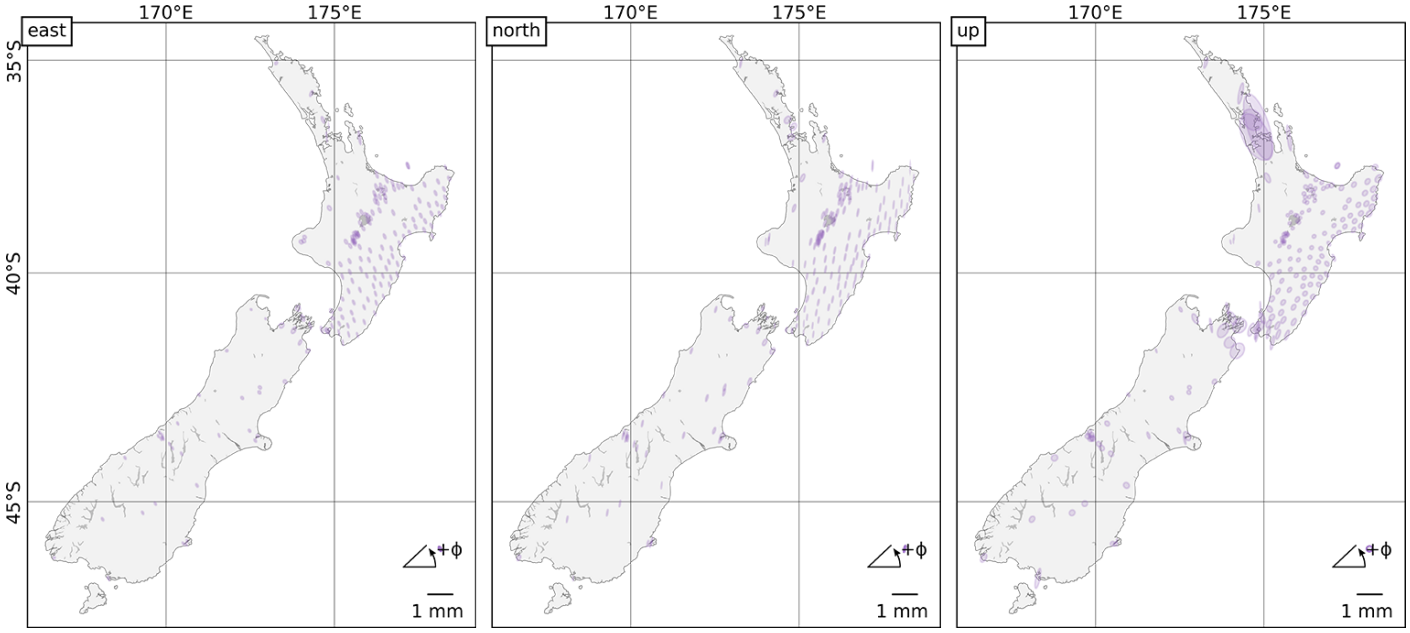

Figure S3. Influence of errors in the ocean-tide models on the modeled OTL values shown as 95% confidence ellipsoids of vector differences between OTL values based on FES2014b, TPXO9.v1 and GOT4.10c ocean tide models. The Green's function was kept fixed to STW105d. The errors were computed separately for in-phase and out-phase components. The scale is consistent with the rest of OTL residuals maps.

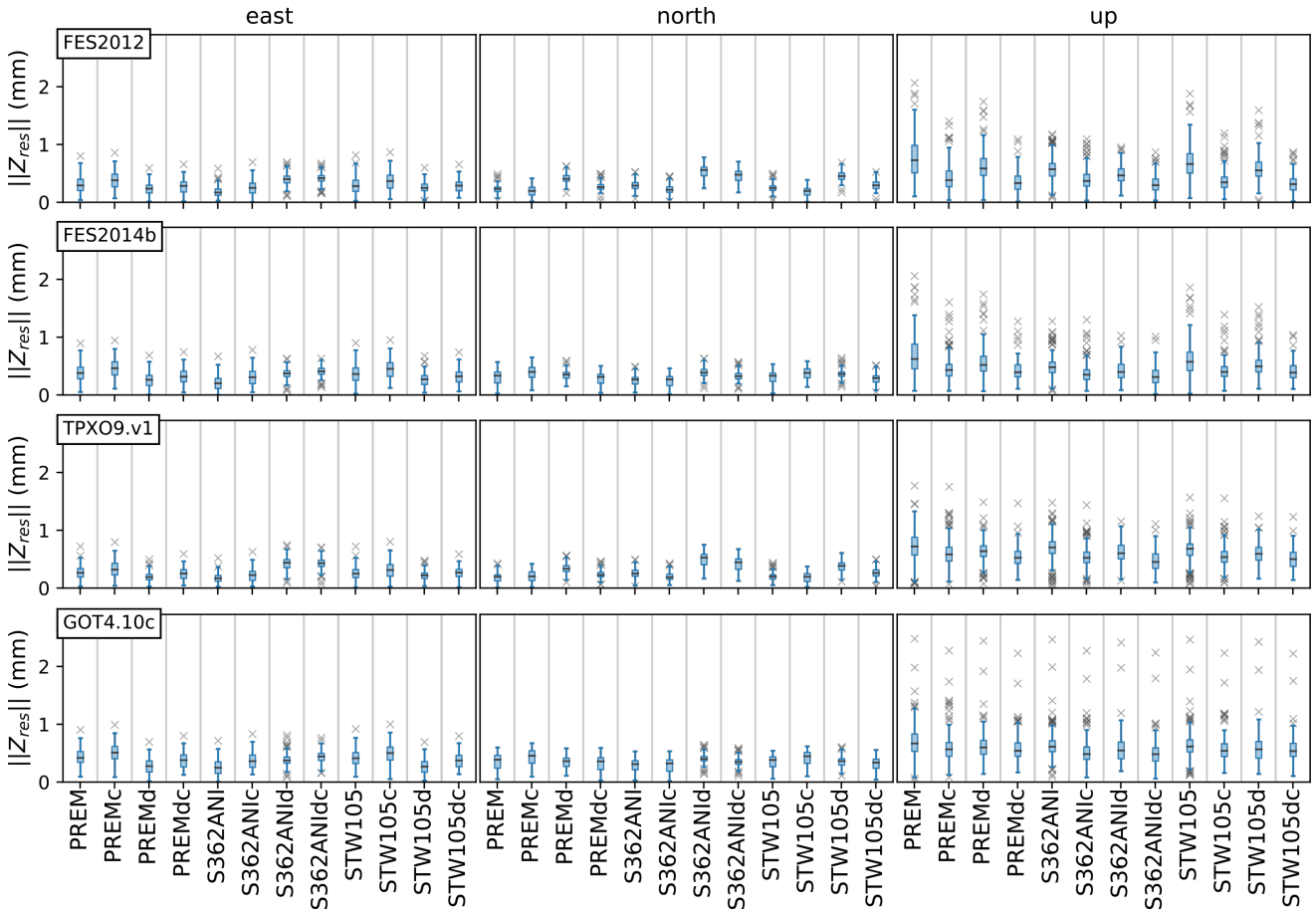

Figure S4. Residual OTL, $\|Z_{res}\|$, relative to (top to bottom) FES2012, FES2014b, TPXO9.v1, GOT4.10c ocean tide models and a set of Green's functions for the east, north and up components (left to right).

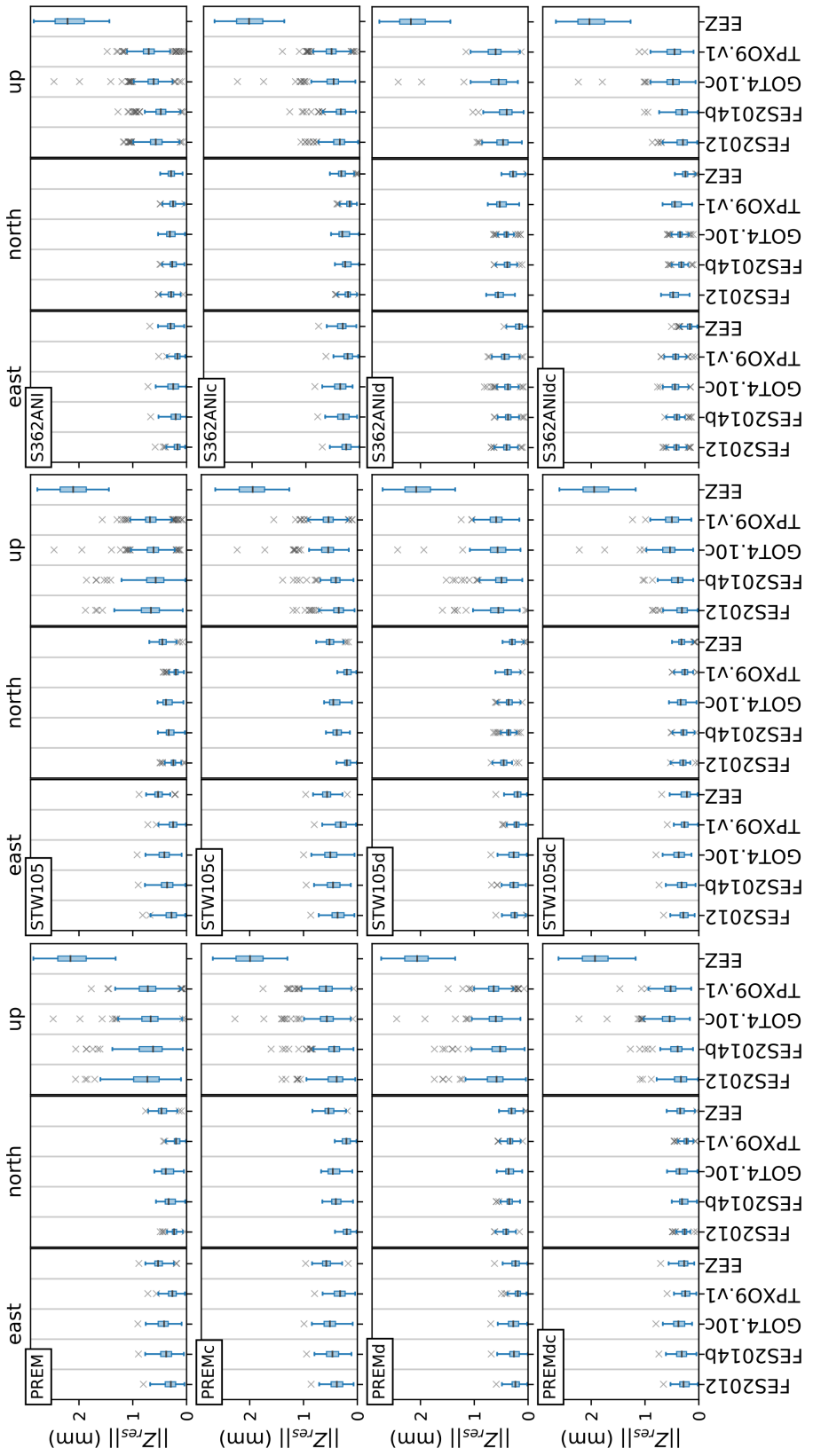

Figure S5. Comparison of FES2012, FES2014b, TPXO9.v1 and GOT4.10c ocean tide models over a range of Green's functions and corrections of compressibility and dissipation.

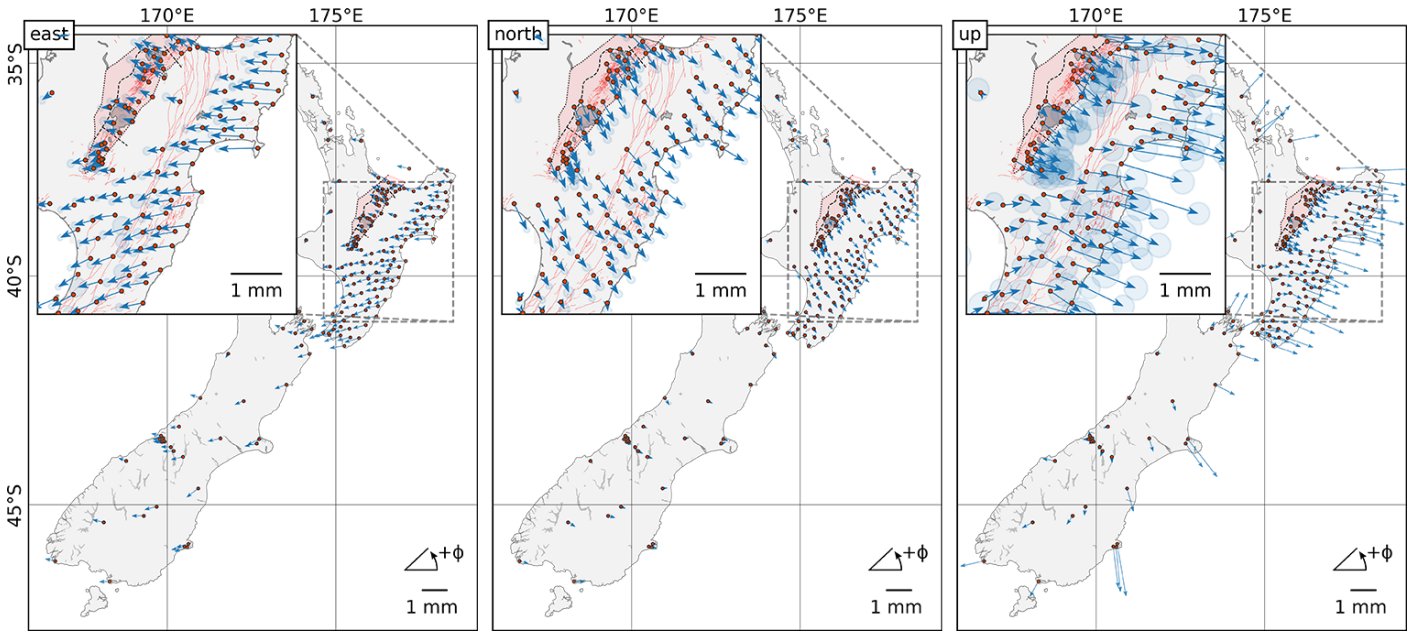

Figure S6.1. Residual OTL, $\|Z_{res}\|$, relative to FES2014b ocean tide model and PREM Green's function in the east, north and up components.

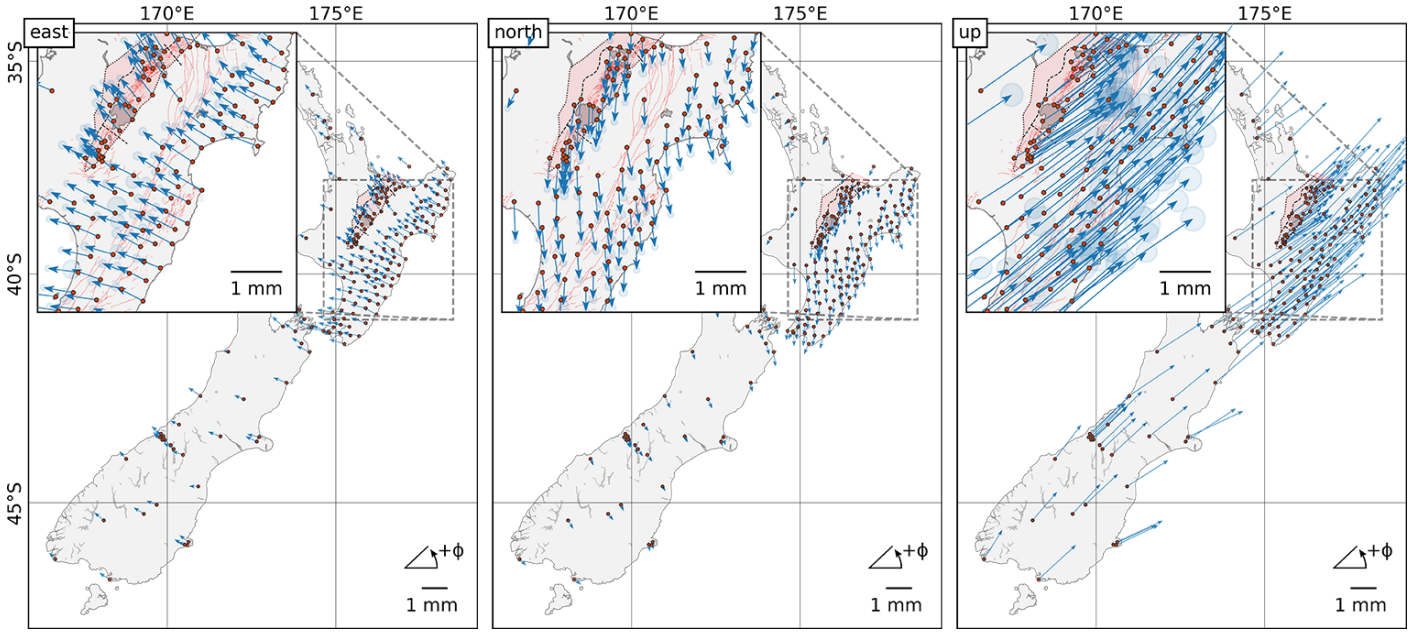

Figure S6.2. Residual OTL, $\|Z_{res}\|$, relative to EEZ regional ocean tide model (FES2014b outside EEZ's coverage) and PREM Green's function in the east, north and up components.

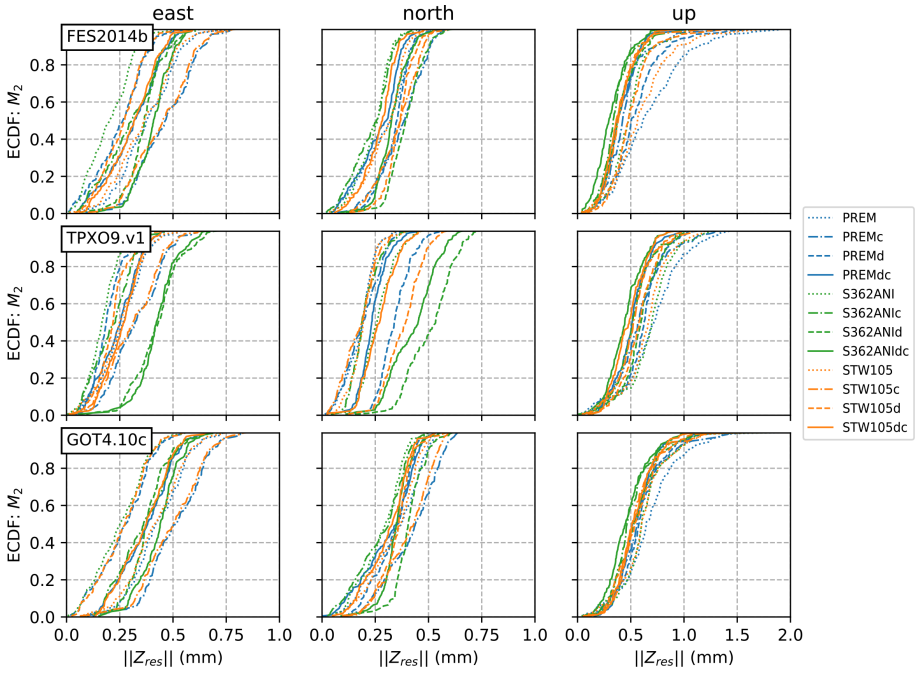

Figure S7.1. ECDF plots for three recent global ocean tide models ocean tide models and a set of Green's functions for the east, north and up components.

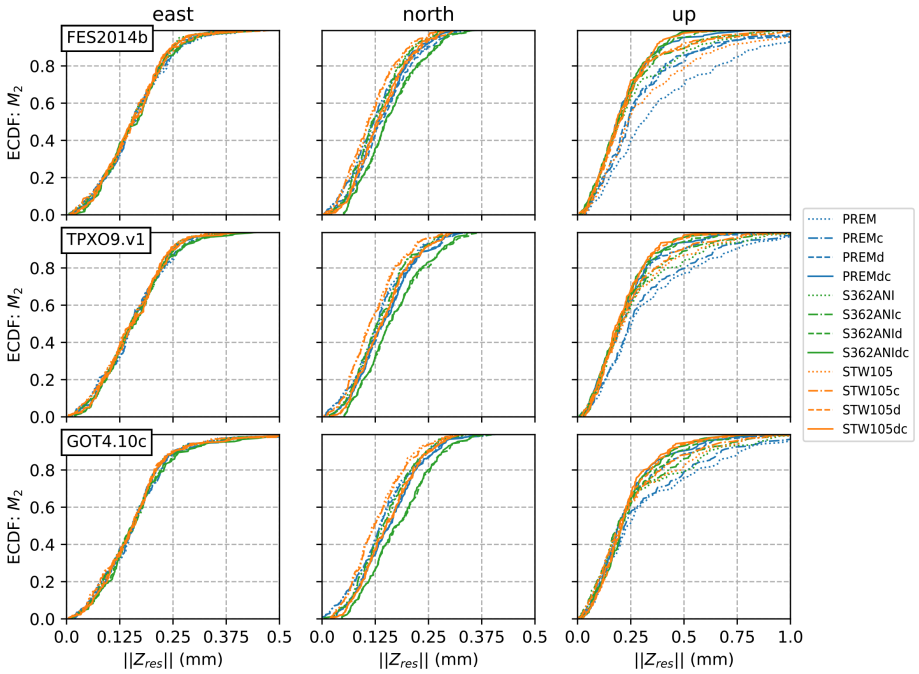

Figure S7.2. Same as Figure S7.1 but with mean residual OTL vector removed for each set of modeled values for the east, north and up components.

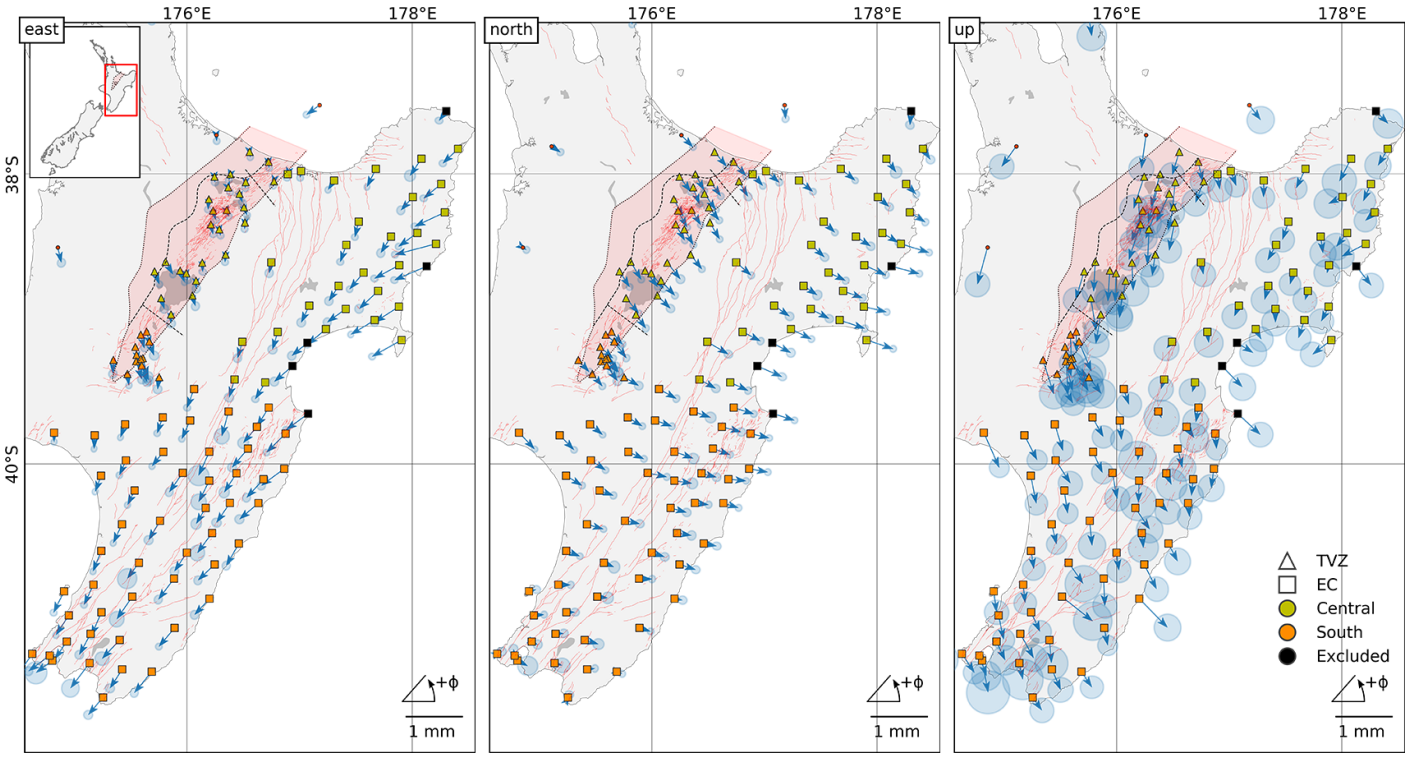

Figure S8. GPS-derived M_2 OTL residuals for a section of the North Island using FES2014b_STW105dc for east, north and up components. Sites are categorized into Taupo Volcanic Zone (TVZ) and East Coast (EC) regions (symbol shape) with subdivision of each into central and south along the TVZ central/south boundary (symbol color).

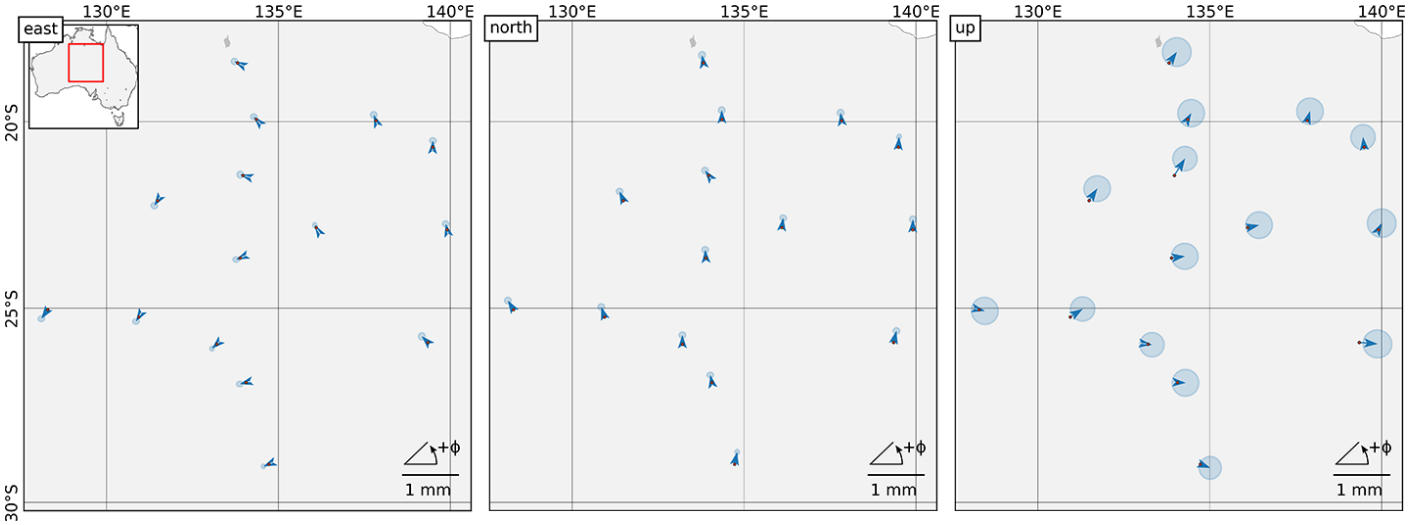

Figure S9. Residual OTL, $\|Z_{res}\|$, relative to FES2014b ocean tide model and STW105d Green's function (maximum bias in New Zealand dataset) for the east, north and up components derived at 14 inland Australian sites.

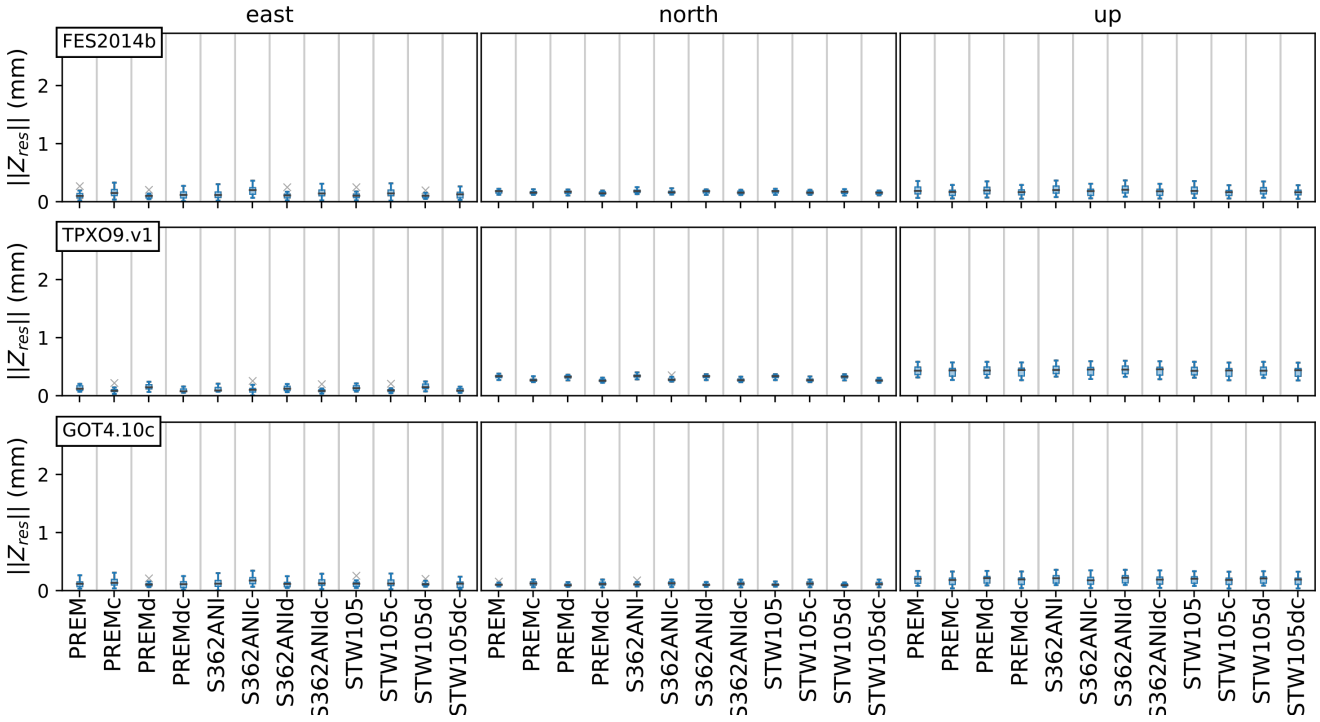

Figure S10. Residual OTL, $\|Z_{res}\|$, derived in the inland Australia relative to FES2014b, TPXO9.v1, GOT4.10c ocean tide models and a set of Green's functions for the east, north and up components.

Table S5. M_2 amplitude differences computed over 15 tide gauges relative to a set of ocean tide models. The bottom row shows an average amplitude difference per ocean tide model. The low value of FES2004 is associated with a low tide anomaly in the Hauraki Gulf. All values in meters.

TG	FES2004	FES2012	FES2014b	GOT4.10c	TPXO9	EEZ
AUCT	0.3371	1.0155	1.0042	0.8271	1.1103	1.2265
CHST	1.1169	1.0863	1.1056	1.1116	1.0897	1.1643
CPIT	0.6303	0.6275	0.6262	0.6199	0.6247	0.6642
GBIT	0.7730	0.7797	0.7895	0.8643	0.7698	0.8007
GIST	0.6313	0.6313	0.6316	0.6405	0.6305	0.6496
KAIT	0.6583	0.6423	0.6515	0.6405	0.6375	0.7078
LOTT	0.6947	0.7008	0.6946	0.7015	0.6933	0.7097
MNKT	1.1792	1.0872	1.0914	1.1545	1.0806	1.2510
NAPT	0.6694	0.6659	0.6595	0.6815	0.6476	0.7001
NCPT	0.7950	0.8070	0.7990	0.8021	0.7972	0.8150
OTAT	0.6939	0.7194	0.7179	0.7375	0.7590	0.7931
PUYT	0.7747	0.7782	0.7901	0.7604	0.7639	0.8394
SUMT	0.7838	0.8530	0.8481	0.8143	0.8235	0.9054
TAUT	0.7291	0.7177	0.7224	0.7225	0.7183	0.7566
WLGT	0.6251	0.3819	0.3809	0.3030	0.4199	0.5130
Avg. difference (m)	-0.0080	0.0295	0.0305	0.0113	0.0232	0.0841

Table S6. Q-values profiles* for PREM and STW105.

PREM

Depth (km)	Q
600.0	143.0
400.0	143.0
220.0	80.0
80.0	600.0
24.4	600.0
15.0	600.0

STW105

Depth (km)	Q
600.0	165.0
410.0	165.0
220.0	70.0
120.0	200.0
30.0	200.0
24.4	300.0
15.0	300.0

* from depth 220-80km PREM uses a Q of 80 and from a depth of 220-120km, STW105 uses a Q of 70. The last layer goes from a depth of 15km to the surface. No information is provided by the authors of either model on the uncertainty of Q values.

Table S7. Average residual amplitude (A) and phase (ϕ) values per each block. "c" and "s" indices stand for central and south blocks.

	TVZ_c		TVZ_s		EC_c		EC_s	
	A, mm	$\phi, ^\circ$	A, mm	$\phi, ^\circ$	A, mm	$\phi, ^\circ$	A, mm	$\phi, ^\circ$
east	0.15	-83.31	0.29	-78.61	0.37	-127.69	0.39	-122.87
north	0.32	-53.03	0.30	-43.96	0.33	-30.85	0.25	-8.62
up	0.51	-102.07	0.51	-70.29	0.26	-109.60	0.36	-71.66